

Analytic solution to degenerate biphoton states generated in arrays of nonlinear waveguides

Jefferson Delgado-Quesada,^{1,2} David Barral,³ Kamel Bencheikh,⁴ and Edgar A. Rojas-González^{1,2,*}

¹*Centro de Investigación en Ciencia e Ingeniería de Materiales, Universidad de Costa Rica, Costa Rica*

²*Escuela de Física, Universidad de Costa Rica, Costa Rica*

³*Galicia Supercomputing Center (CESGA), Avda. de Vigo S/N, Santiago de Compostela, 15705, Spain*

⁴*Centre de Nanosciences et de Nanotechnologies, CNRS,*

Université Paris-Saclay, 91120 Palaiseau, France

(Dated: December 2, 2024)

Waveguide arrays are a powerful platform for studying and manipulating quantum states of light. When nonlinearity arises due to a spontaneous parametric down-conversion process, the degree of entanglement can increase, contrary to a linear array, enabling the generation of nonclassical biphoton states—which are a valuable resource for various quantum technologies. In this work, we employed a supermodes approach to obtain an analytic solution for the evolution of degenerate biphoton states under the undepleted pump approximation. We examined the general features of our solution, including results for small arrays, propagation when only one waveguide is pumped, and the inversion problem of a target output state. Analytic results offer valuable physical insights into the propagation of light in arrays of nonlinear waveguides, and enable the determination of the initial conditions required to achieve a desired quantum state—for example, the injection pump profile. In general, such calculations can be computationally demanding for large arrays. However, the numerical implementation of the proposed method scales efficiently—both for the direct, and inverse problems. In future work, our approach could be extended to non-degenerate biphoton states. Also, it could be applied in the study of diffusion regimes, the introduction of disorder, and the development of reliable optimization methods for inverting arbitrary output states.

I. INTRODUCTION

Integrated photonics platforms are key for the development of quantum technologies [1]. Particularly, they are able to generate, process, and detect quantum states of light in compact optical chips. An important example is an array of nonlinear waveguides (ANW) [2], which combines coupling and nonlinear effects to manipulate an input quantum state. An ANW can be implemented by fabricating the waveguides with nonlinear materials, such as periodically poled lithium niobate (PPLN) [3].

The importance of the nonlinearity comes from the fact that ANWs are able to increase the degree of entanglement of an input state, in contrast to its linear version, which in the best-case scenario can only preserve it [4].

The properties of ANWs have been investigated both in the continuous [5–8] and discrete variable regimes. Particularly, in the discrete variable context, biphoton states in ANWs have been studied in relation to different topics; such as, quantum walk [4], topological photonics [9, 10], Anderson localization [11], engineering of spatio-spectral correlations [3, 12], and the generation of nonclassical states [4].

In addition, nonclassical biphoton states in multimode systems, such as those that can be produced in ANWs, could be key resources for diverse integrated photonic quantum technologies. For example, quantum communication [13], quantum computing [14], and distributed quantum sensing [15].

The output states in ANW can be readily obtained numerically for a given set of input parameters [3, 4, 7]. However, the inverse problem is challenging. That is, determining the input conditions to engineer a particular desired output state. Interesting and valuable steps have been taken in this direction.

Particularly, Belsley et al. [16] make use of the Cayley-Hamilton theorem to obtain analytic expressions that describe the biphoton output states in ANWs as well as an inversion method that expresses the input conditions in terms of the output state.

In addition, He et al. [17] propose to build the scattering tensor, which describes the propagation in ANWs, and compute its pseudo-inverse to obtain the input parameters that approximate a desired output biphoton state.

Belsley et al. [16] consider the undepleted pump approximation, negligible coupling of the pump photons, and non-degenerate signal and idler photons. On the other hand, the treatment of He et al. [17] takes into account pump depletion effects, pump coupling, and near-degenerate signal and idler photons. Both works assume a flat coupling profile.

The methods commented above may work efficiently in ANW with few waveguides. However, they could be computationally demanding for large arrays.

In this work, we propose to use the supermodes approach presented in Barral et al. [18] to obtain an analytic solution for the degenerate biphoton states produced in ANWs of an arbitrary number of waveguides, and a general coupling profile. An analytic expression presents two main advantages. First, it gives insight into

* edgar.rojasgonzalez@ucr.ac.cr

the physics of ANWs. Second, having the output state as an explicit function of the input parameters provides the possibility of implementing optimization algorithms to obtain the input conditions required to generate a desired target state, or at least to get the best possible approximation.

The structure of this article is the following. First, in Sec. II we introduce the relevant parameters that describe the propagation in an ANW. Second, in Sec. III we obtain an analytic solution to the propagation problem. Third, in Sec. IV we comment on the general properties of this solution. Next, in Sec. V, we present some application examples. Then, in Sec. VI, we give a proof of principle demonstration of the use of the analytic solution in an inverse problem. Finally, we summarize the main results, and provide some relevant remarks.

II. ANW AND INPUT PARAMETERS

A schematic of the ANW model is depicted in Fig. 1. It consists of N identical waveguides with a quadratic nonlinearity described by the second-order susceptibility $\chi^{(2)}$. Each waveguide has a specific injection. Particularly, the j th waveguide is injected with a strong coherent pump field $\alpha_j = |\alpha_j|e^{i\phi_j}$. In these circumstances, a spontaneous parametric down-conversion (SPDC) process can take place in the ANW. Here, we consider a situation in which the undepleted pump approximation is valid, and focus on the degenerate case. That is, the instance in which a pump photon with frequency ω_p is down-converted into two twin signal photons with frequency $\omega_s = \omega_p/2$.

Another process that can take place in the ANW is evanescent coupling between waveguides. Here, we consider only nearest-neighbor coupling of the signal photons. The confinement increases with the frequency [19]. Thus, for the studied propagation lengths, we assume the pump photons remain in their initial waveguide because their coupling is considered negligible compared to that of the signal photons.

The spatial evolution in the ANW is governed by the momentum operator \hat{M} [20]. Under the conditions described above, \hat{M} can be expressed in the interaction picture as follows [21]

$$\hat{M} = \hbar \sum_{j=1}^{N-1} C_j \hat{A}_{j+1} \hat{A}_j^\dagger e^{i[\beta_{j+1}(\omega_s) - \beta_j(\omega_s)]z} + \hbar \sum_{j=1}^N \eta_j (\hat{A}_j^\dagger)^2 e^{i[\beta_j(\omega_p) - 2\beta_j(\omega_s)]z} + \text{h.c.}, \quad (1)$$

with h.c. denoting the Hermitian conjugate, $\beta_j(\omega)$ the propagation constant at the j th waveguide and frequency ω , and \hat{A}_j (\hat{A}_j^\dagger) the monochromatic slowly-varying amplitude annihilation (creation) operator associated with the signal photons in mode j (the j th

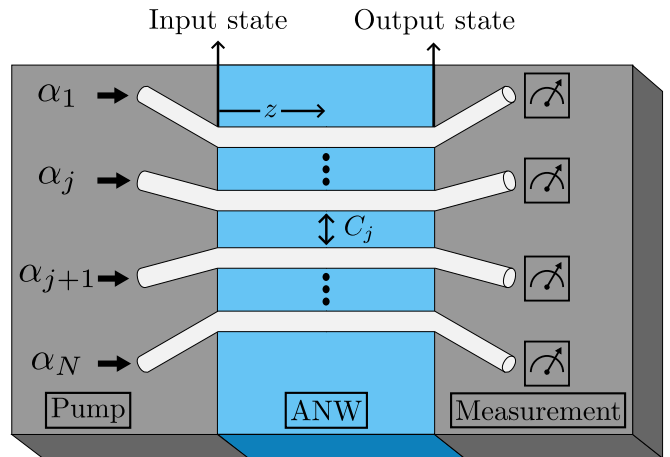


FIG. 1. Schematic of the ANW with N identical waveguides. The j th waveguide is injected with the pump field α_j . The linear coupling, and nonlinear effects take place only within the ANW region. The propagation occurs along the z axis, and $z = 0$ (related to the input state $|\Psi(0)\rangle$) corresponds to the beginning of the ANW region. The linear coupling between waveguides j and $j + 1$ is characterized by the parameter C_j , and the nonlinear effects are determined by the nonlinear constant g —which, in this case, is the same for all waveguides. The output state is taken at the end of the ANW region. The output of each individual waveguide could be measured, distributed, or sent as an input of a certain operation.

waveguide). These operators depend on the position, and frequency. In addition, they satisfy the commutation relation $[\hat{A}_j(z, \omega), \hat{A}_{j'}^\dagger(z', \omega')] = \delta(z, z')\delta(\omega - \omega')\delta_{j, j'}$ [22], with z the direction of propagation along the ANW. The first term in Eq. (1) describes the coupling between neighboring waveguides, with $C_j \equiv f_j C_0$ the linear coupling constant between waveguide j and $j + 1$, C_0 a characteristic coupling strength, and f_j a real scaling factor. Here, the coupling is considered to be constant along the propagation direction. The second term in Eq. (1) represents the SPDC process, with $\eta_j \equiv g\alpha_j = |\eta_j|e^{i\phi_j}$ the nonlinear coupling constant related to the j th waveguide, and g a nonlinear constant which determines the strength of the nonlinear process—it is proportional to $\chi^{(2)}$, and the overlap between the pump and signal fields. In general, g and C_0 are frequency-dependent, and we consider them to be real (note that this assumption does not affect the underlying physics of the problem).

In this work, we focus on the case of identical waveguides ($\beta_j(\omega) \equiv \beta(\omega)$ for any j), and assume the phase matching condition $\beta(\omega_p) = 2\beta(\omega_s)$ is satisfied within the propagation region. Hence, Eq. (1) simplifies to

$$\hat{M} = \hbar \sum_{j=1}^{N-1} C_j \hat{A}_{j+1} \hat{A}_j^\dagger + \hbar \sum_{j=1}^N \eta_j (\hat{A}_j^\dagger)^2 + \text{h.c.}, \quad (2)$$

III. PROPAGATION PROBLEM IN THE ANW

In the ANW, the output state $|\Psi(z)\rangle$ at a propagation distance z can be obtained by

$$|\Psi(z)\rangle = \hat{O} \left[e^{\frac{i}{\hbar} \int_0^z \hat{M} dz'} \right] |\Psi(0)\rangle, \quad (3)$$

with $|\Psi(0)\rangle$ the input state at $z = 0$, which in our case corresponds to the vacuum state $|0\rangle$. Here, \hat{O} denotes a space-ordering operator, which is required because, in general, \hat{M} does not commute with itself at different positions. However, the space-ordering effects can be neglected in the low-injection regime [23], which is the case in this work. As a result, we can write

$$|\Psi(z)\rangle = e^{\frac{i}{\hbar} \int_0^z \hat{M} dz'} |\Psi(0)\rangle. \quad (4)$$

Next, we will transform the problem into a convenient basis. We begin by expressing the momentum operator in the following compact form

$$\hat{M} = \hbar(A_D^T \Omega A + A_D^T P A_D + A^T P^\dagger A), \quad (5)$$

with $A \equiv (\hat{A}_1, \dots, \hat{A}_N)^T$, $A_D \equiv (\hat{A}_1^\dagger, \dots, \hat{A}_N^\dagger)^T$, P the diagonal matrix $P \equiv \text{diag}(\eta_1, \dots, \eta_N)$, and Ω a real, symmetric, and tridiagonal matrix of the form

$$\Omega = \begin{pmatrix} 0 & C_1 & & & \\ C_1 & 0 & C_2 & & \\ & C_2 & \ddots & \ddots & \\ & & \ddots & \ddots & C_{N-1} \\ & & & C_{N-1} & 0 \end{pmatrix}. \quad (6)$$

The linear supermodes basis $\{\hat{b}_j\}$ corresponds to the propagation eigenmodes of the ANW [24]. It diagonalizes the problem with just linear coupling effects. That is, a case in which we can consider P as a null matrix (for example, taking $g = 0$). The transformation from the physical $\{\hat{A}_j\}$ to the supermodes basis $\{\hat{b}_j\}$ can be expressed as follows

$$b = SA, \quad (7)$$

with $b \equiv (\hat{b}_1, \dots, \hat{b}_N)^T$, and S an orthogonal transformation matrix of the form

$$S = \begin{pmatrix} |v_1\rangle^T \\ \vdots \\ |v_N\rangle^T \end{pmatrix}, \quad (8)$$

with $|v_k\rangle$ the k th normalized eigenvector of Ω associated with the eigenvalue λ_k . Due to the nature of Ω

stated above, its eigenvalues are real, and possesses a set of N orthogonal eigenvectors, which can be defined as real [25].

In this work, the indexing of the eigenvalues was chosen in such a way that $\lambda_1 > \dots > \lambda_k > \dots > \lambda_N$.

The following relations can be obtained from Eq. (7)

$$\hat{b}_k = \sum_{j=1}^N S_{kj} \hat{A}_j, \quad (9)$$

$$\hat{A}_k = \sum_{j=1}^N S_{jk} \hat{b}_j. \quad (10)$$

As an intermediate step, we would like to express $|\Psi(z)\rangle$ in terms of the supermodes basis $\{\hat{b}_k\}$. Thus, the momentum operator \hat{M} defined in Eq. (1) can be written in the following way by means of the relation given in Eq. (10)

$$\hat{M} = \hat{M}_L + \hat{M}_{NL}, \quad (11)$$

with

$$\hat{M}_L = \hbar \sum_{j=1}^N \lambda_j \hat{b}_j^\dagger \hat{b}_j, \quad (12)$$

the term corresponding to the linear coupling effects (which is diagonal in the supermodes basis), and

$$\hat{M}_{NL} = \hbar \left\{ \sum_{n,m=1}^N \sum_{j=1}^N \eta_j S_{nj} S_{mj} \hat{b}_n^\dagger \hat{b}_m^\dagger + \text{h.c.}, \right\} \quad (13)$$

the term related to the nonlinear coupling.

The Eqs. (11), (12), and (13) illustrate the main characteristics of light propagation in ANWs. That is, the first, and second terms on the right-hand side of Eq. (11) represent, respectively, the linear coupling between waveguides described as a superposition of supermodes, and the coupling between supermodes due to the nonlinear effects.

Note that \hat{M}_L , with the form given in Eq. (12), corresponds to the free-rotating part of \hat{M} in the linear supermodes basis. Hence, it is natural to change to the interaction picture, and obtain

$$|\Psi(z)\rangle_I = \exp \left[\frac{i}{\hbar} \int_0^z \hat{M}_{NL}^{(I)}(z') dz' \right] |0\rangle, \quad (14)$$

with $|\Psi(z)\rangle_I = \exp(-i\hat{M}_L z/\hbar) |\Psi(z)\rangle$, and

$$\begin{aligned} \hat{M}_{NL}^{(I)}(z) &= \hbar \sum_{n,m=1}^N \sum_{j=1}^N |\eta_j| S_{nj} S_{mj} \hat{B}_n^\dagger \hat{B}_m^\dagger e^{i\phi_j} e^{-i(\lambda_n + \lambda_m)z} \\ &+ \text{h.c.}, \end{aligned} \quad (15)$$

with $\hat{B}_k = \hat{b}_k^{(1)} e^{-i\lambda_k z}$ the slowly-varying amplitude part of the supermodes in the interaction picture, $\hat{b}_k^{(1)}$. As a result

$$\int_0^z \hat{M}_{\text{NL}}^{(1)}(z) dz' = \hbar \sum_{n,m=1}^N K_{nm}(z) e^{-i(\lambda_n + \lambda_m)z} \hat{B}_n^\dagger \hat{B}_m^\dagger + \text{h.c.}, \quad (16)$$

with

$$K_{nm}(z) = z \sum_{j=1}^N \{ |\eta_j| S_{nj} S_{mj} e^{i\phi_j} e^{i(\lambda_n + \lambda_m)z/2} \times \text{sinc}[(\lambda_n + \lambda_m)z/2] \} \quad (17)$$

the nm entry of a symmetric matrix $K(z)$, which can be expressed as

$$K(z) = \tilde{P} \odot T(z), \quad (18)$$

with \odot denoting a Hadamard product (that is, an entrywise product between two matrices with the same dimensions),

$$\tilde{P} = S P S^T, \quad (19)$$

and $T(z)$ a matrix with nm entries defined as

$$T_{nm}(z) = z e^{i(\lambda_n + \lambda_m)z/2} \text{sinc}[(\lambda_n + \lambda_m)z/2]. \quad (20)$$

The result from Eq. (16) can be plugged into Eq. (14), which gives the following expression for the output state in the interaction picture

$$|\Psi(z)\rangle_{\text{I}} = \exp \left\{ i \left[\sum_{n,m=1}^N K_{nm}(z) \hat{B}_n^\dagger \hat{B}_m^\dagger e^{-i(\lambda_n + \lambda_m)z} + \text{h.c.} \right] \right\} |0\rangle. \quad (21)$$

It is possible to return to $|\Psi(z)\rangle$, in the basis $\{\hat{b}_k\}$, by means of the relation

$$\begin{aligned} |\Psi(z)\rangle &= \exp \left(i \hat{M}_{\text{L}} z / \hbar \right) |\Psi(z)\rangle_{\text{I}} \\ &= \exp \left[i z \sum_{j=1}^N \lambda_j \hat{b}_j^\dagger \hat{b}_j \right] |\Psi(z)\rangle_{\text{I}}. \end{aligned} \quad (22)$$

Thus, $|\Psi(z)\rangle$ can be expressed at first order in η_j as follows

$$\begin{aligned} |\Psi(z)\rangle &= \left[1 + i \sum_{n,m=1}^N K_{nm}(z) \hat{b}_n^\dagger \hat{b}_m^\dagger \right] |0\rangle \quad (23) \\ &= |0\rangle + \sum_{n=1}^N \tilde{K}_{nn}(z) |\dots, 2_n, \dots\rangle_{\text{b}} \\ &\quad + \sum_{n=1}^{N-1} \sum_{m=n+1}^N \tilde{K}_{nm}(z) |\dots, 1_n, \dots, 1_m, \dots\rangle_{\text{b}}, \end{aligned} \quad (24)$$

defining a matrix $\tilde{K}(z)$ with nm entries given by $\tilde{K}_{nm}(z) = i 2^{1-\delta_{nm}/2} K_{nm}(z)$, with δ_{nm} the Kronecker delta with indexes nm .

In this way, the amplitudes of the $|\dots, 1_n, \dots, 1_m, \dots\rangle_{\text{b}}$, and $|\dots, 2_n, \dots\rangle_{\text{b}}$ biphoton eigenstates in the supermodes basis are given by $\tilde{K}_{nm}(z)$ (with $n \neq m$), and $\tilde{K}_{nn}(z)$, respectively.

It is worth mentioning we are interested in biphoton states. Hence, we assume to be working in a low-injection regime such that the approximation done in Eq. (23) is valid.

Equation (24) gives an analytic expression of the output biphoton state in the supermodes basis, and this will be used later in this work.

The corresponding output state in the physical basis can be obtained from Eq. (23) by means of the relation given in Eq. (9), and it can be written as follows

$$|\Psi(z)\rangle = |0\rangle + i \sum_{k,q=1}^N D_{kq}(z) \hat{A}_k^\dagger \hat{A}_q^\dagger |0\rangle, \quad (25)$$

with

$$\begin{aligned} D_{kq}(z) &= \sum_{n,m=1}^N S_{kn}^T K_{nm}(z) S_{mq} \\ &= \sum_{j,n,m=1}^N |\eta_j| e^{i\phi_j} S_{nj} S_{mj} S_{nk} S_{mq} T_{nm}(z). \end{aligned} \quad (26)$$

In fact, the output state in the physical basis can be expressed as

$$\begin{aligned} |\Psi(z)\rangle &= |0\rangle + \sum_{q=1}^N \tilde{D}_{qq}(z) |\dots, 2_q, \dots\rangle \\ &\quad + \sum_{k=1}^{N-1} \sum_{q=k+1}^N \tilde{D}_{kq}(z) |\dots, 1_k, \dots, 1_q, \dots\rangle, \end{aligned} \quad (27)$$

with \tilde{D} a matrix with kq entries $\tilde{D}_{kq}(z) = i 2^{1-\delta_{kq}/2} D_{kq}(z)$.

Thus, the amplitudes of the biphoton states in the physical basis correspond simply to the entries of the matrix \tilde{D} with form

$$\tilde{D}(z) = S^T \tilde{K}(z) S. \quad (28)$$

IV. GENERAL PROPERTIES OF THE SOLUTION

The light propagation in the ANW is, to a large extent, governed by the characteristics of the eigenvalues and eigenvectors of the matrix Ω .

The nature of Ω , as defined in Eq. (6), imposes special properties on its eigenvalue spectrum $\{\lambda_k\}$, and the corresponding set of eigenvectors $\{|v_k\rangle\}$ [25]. Some of these are stated below.

First, the set of eigenvectors is orthonormal, thus

$$\sum_{k=1}^N S_{nk} S_{mk} = \delta_{nm}, \quad (29)$$

$$\sum_{k=1}^N S_{kn} S_{km} = \delta_{nm}. \quad (30)$$

Second, the following relations are satisfied between eigenvalues, and eigenvectors with indexes symmetric with respect to the center of the set $\{1, \dots, N\}$ (for example, k and $N + 1 - k$)

$$\lambda_{N+1-k} = -\lambda_k, \quad (31)$$

$$S_{N+1-k,m} = (-1)^{m+1} S_{km}. \quad (32)$$

Hereinafter, we will denote the pair of supermodes with indexes k and $N + 1 - k$ as a centrosymmetric pair.

In addition, Eqs. (29) and (32) can be combined to obtain the relations

$$\sum_{k=1}^N (-1)^{k+1} S_{nk} S_{mk} = \delta_{n,N+1-m}, \quad (33)$$

$$\sum_{k=1}^{\lceil N/2 \rceil} S_{n,2k-1} S_{m,2k-1} = \frac{1}{2} (\delta_{nm} + \delta_{n,N+1-m}), \quad (34)$$

$$\sum_{k=1}^{\lceil N/2 \rceil} S_{n,2k} S_{m,2k} = \frac{1}{2} (\delta_{nm} - \delta_{n,N+1-m}), \quad (35)$$

with $\lceil x \rceil$ denoting the ceiling function—that is, the smallest integer greater than or equal to x .

A. Supermodes phase-matching

The amplitudes of the output biphoton eigenstates in the supermodes basis $\tilde{K}_{nm}(z)$ are proportional to

$\text{sinc}[(\lambda_n + \lambda_m)z/2]$ —see Eqs. (17) and (24). This is a phase-matching factor which determines the eigenstates (in the supermodes basis) that become dominant in the output state as the propagation distance z increases. That is, those with $|\lambda_n + \lambda_m|$ as small as possible.

Particularly, the limiting case is obtained when $\lambda_n + \lambda_m = 0$, which is a condition satisfied by centrosymmetric pairs of supermodes (with $m = N + 1 - n$). Thus, the dominant eigenstates are those with form $|\dots, 1_n, \dots, 1_{N+1-n}, \dots\rangle_b$.

An ANW with odd size N possesses a supermode with a vanishing eigenvalue, which we denote here as the zero supermode. According to the relation given in Eq. (31), this corresponds to the central supermode associated with the index $(N + 1)/2$. Evidently, the condition $\lambda_n + \lambda_m = 0$ is satisfied for the central supermode when $n = m = (N + 1)/2$, and this is related to an eigenstate of the form $|\dots, 2_{(N+1)/2}, \dots\rangle_b$.

In summary, as the propagation increases the output state in the supermodes basis will be dominated by the eigenstates stated above.

B. Simple solutions: Symmetric injection profiles

As mentioned elsewhere [18], it is possible to choose certain symmetric injection profiles which, due to the relations in Eqs. (30)-(35), give rise to a significant simplification of the analytic expression for the output state.

To the best of our knowledge, the most notable simplification is obtained when the injection is identical for all the odd (even) waveguides. That is, with nonlinear coupling constants given by

$$\eta_j = \begin{cases} |\eta_1| e^{i\phi_1}, & \text{if } j \text{ is odd,} \\ |\eta_2| e^{i\phi_2}, & \text{if } j \text{ is even.} \end{cases} \quad (36)$$

In this case, we can arrange Eq. (17) and use the relations in Eqs. (34) and (35) to obtain

$$\begin{aligned} K_{nm}(z) &= \left[|\eta_1| e^{i\phi_1} \left(\sum_{k=1}^{\lceil N/2 \rceil} S_{n,2k-1} S_{m,2k-1} \right) \right. \\ &\quad \left. + |\eta_2| e^{i\phi_2} \left(\sum_{k=1}^{\lceil N/2 \rceil} S_{n,2k} S_{m,2k} \right) \right] T_{nm} \\ &= \left[\frac{1}{2} |\eta_1| e^{i\phi_1} (\delta_{nm} + \delta_{n,N+1-m}) \right. \\ &\quad \left. + \frac{1}{2} |\eta_2| e^{i\phi_2} (\delta_{nm} - \delta_{n,N+1-m}) \right] T_{nm} \\ &= F_A T_{nm} \delta_{nm} + F_B T_{nm} \delta_{n,N+1-m}, \quad (37) \end{aligned}$$

with

2. Simple solution in the physical basis

$$F_A \equiv \frac{1}{2}(|\eta_1|e^{i\phi_1} + |\eta_2|e^{i\phi_2}), \quad (38)$$

$$F_B \equiv \frac{1}{2}(|\eta_1|e^{i\phi_1} - |\eta_2|e^{i\phi_2}). \quad (39)$$

1. Simple solution in the supermodes basis

The result from Eq. (37) can be plugged into Eq. (23) to obtain the following simplified solution in the supermodes basis

$$|\Psi(z)\rangle = |0\rangle + iz\sqrt{2}F_A \sum_{n=1}^N e^{i\lambda_n z} \text{sinc}(\lambda_n z) |\dots, 2_n, \dots\rangle_b \\ + 2izF_B \sum_{n=1}^{\lfloor N/2 \rfloor} |\dots, 1_n, \dots, 1_{N+1-n}, \dots\rangle_b. \quad (40)$$

with $\lfloor x \rfloor$ denoting the floor function—that is, the greatest integer smaller than or equal to x .

The output state given in Eq. (40) presents interesting physical properties.

First, the eigenstates with mixed supermodes of the form $|\dots, 1_n, \dots, 1_m, \dots\rangle_b$ ($n \neq m$) show nonvanishing amplitudes only for pairs of centrosymmetric supermodes with $m = N + 1 - n$.

Second, the antibunching condition in the supermodes basis is obtained when $F_A = 0$, which is satisfied when $|\eta_1| = |\eta_2|$ and $\phi_1 = \phi_2 + 2\pi(m + 1/2)$, with $m \in \mathbb{Z}$ —note we are not considering the trivial solution $|\eta_1| = |\eta_2| = 0$.

Third, the bunching case in the supermodes basis occurs when $F_B = 0$. That is, for $|\eta_1| = |\eta_2|$ and $\phi_1 = \phi_2 + 2\pi m$, with $m \in \mathbb{Z}$. In the resulting bunching output state, the amplitudes of the eigenstates $|\dots, 2_n, \dots\rangle_b$ are proportional to the factor $\text{sinc}(\lambda_n z)$. Thus, in an odd array, all the probabilities associated with the eigenstates decrease with the propagation z except from that of $|\dots, 2_{(N+1)/2}, \dots\rangle_b$ —corresponding to the zero supermode—because it is the only one that satisfies the phase-matching condition described in section IV A. Hence, for a sufficiently large z , the bunching output state in an odd array would practically resemble $|\dots, 2_{(N+1)/2}, \dots\rangle_b$ —that is, two photons in the zero supermode.

In principle, it is experimentally feasible to move from the physical to the supermodes basis by means of linear transformations [26]—which can be implemented with off-the-shelf optical elements. As a result, the state presented in Eq. (37) could work as a N -mode state from which bunching, and antibunching could be selected only by means of adjusting the relative phase of the injected fields.

The output state in the physical basis equivalent to the expression given in Eq. (40) can be obtained as follows.

We begin by plugging the expression for $K_{nm}(z)$ derived in Eq. (37) into Eq. (26), which gives

$$D_{kq}(z) = \sum_{n,m=1}^N [S_{nk}S_{mq}F_A T_{nm}\delta_{nm} \\ + S_{nk}S_{mq}F_B T_{nm}\delta_{n,(N+1-m)}] \\ = \sum_{n=1}^N [F_A S_{nk}S_{nq}T_{nn} \\ + F_B S_{nk}S_{(N+1-n),q}T_{n,(N+1-n)}] \\ = \sum_{n=1}^N [F_A S_{nk}S_{nq}T_{nn} \\ + (-1)^{q+1}F_B S_{nk}S_{nq}T_{n,(N+1-n)}], \quad (41)$$

where Eq. (32) was used to express $S_{(N+1-n),q}$ in terms of S_{nq} .

Next, from Eqs. (20) and (31) we get $T_{n,(N+1-n)} = z$, which we can plug into Eq. (41) to obtain

$$D_{kq}(z) = F_A \sum_{n=1}^N S_{nk}S_{nq}T_{nn} \\ + (-1)^{q+1}zF_B \left(\sum_{n=1}^N S_{nk}S_{nq} \right) \\ = F_A \sum_{n=1}^N S_{nk}S_{nq}T_{nn} + (-1)^{q+1}zF_B \delta_{kq}, \quad (42)$$

where the orthonormality relation given in Eq. (30) was used to simplify the second term of the right-hand side.

Finally, we plug Eq. (42) into Eq. (27) and get the output state in the physical basis with the form

$$|\Psi(z)\rangle = |0\rangle \\ + i\sqrt{2} \sum_{q=1}^N \left[F_A \left(\sum_{n=1}^N S_{nq}^2 T_{nn} \right) + (-1)^{q+1}zF_B \right] \\ \times |\dots, 2_q, \dots\rangle \\ + i2 \sum_{k=1}^{N-1} \sum_{q=k+1}^N F_A \sum_{n=1}^N S_{nk}S_{nq}T_{nn} \\ \times |\dots, 1_k, \dots, 1_q, \dots\rangle. \quad (43)$$

From Eq. (43) we can see the condition for bunching is $F_A = 0$ —that is, $|\eta_1| = |\eta_2|$, and $\phi_1 = \phi_2 + 2\pi(m + 1/2)$, with $m \in \mathbb{Z}$. Note this corresponds to the antibunching condition in the supermodes basis.

On the other hand, no simple general condition can be obtained for achieving a state in which the two photons can not be detected at the same waveguide—that is, without eigenstates of the form $|\dots, 2_q, \dots\rangle$. This case would need to be studied individually for each particular situation.

It is important to remark that the properties stated here, in relation to the injection profile given in Eq. (36), are general for ANWs of any size N and coupling profile $\{C_j\}$.

V. APPLICATION EXAMPLES

The transformation matrix S takes a simple form when the array is homogeneous—that is, when all the elements of the coupling profile $\{f_j\}$ are equal to one. The elements of the matrix S are [27]

$$S_{nm} = S_{mn} = \frac{\sin\left(\frac{nm\pi}{N+1}\right)}{\sqrt{\sum_{k=1}^N \sin^2\left(\frac{kn\pi}{N+1}\right)}}, \quad (44)$$

while its eigenvalues are given by

$$\lambda_n = 2C_0 \cos\left(\frac{n\pi}{N+1}\right). \quad (45)$$

A. Solution for two waveguides

In the case of a two-waveguide array, the output state in the physical basis, expressed in terms of the entries of the matrix \tilde{D} , is

$$\tilde{D}_{11} = i \frac{2zC_0(\eta_1 - \eta_2) + (\eta_1 + \eta_2) \sin(2C_0z)}{2\sqrt{2}C_0}, \quad (46a)$$

$$\tilde{D}_{12} = \tilde{D}_{21} = \frac{(\eta_1 + \eta_2)[\cos(2C_0z) - 1]}{2C_0}, \quad (46b)$$

$$\tilde{D}_{22} = i \frac{2zC_0(\eta_2 - \eta_1) + (\eta_1 + \eta_2) \sin(2C_0z)}{2\sqrt{2}C_0}. \quad (46c)$$

This is consistent with the results found by Belsley et al. [16]. It is important to remark that the coefficients presented in [16] actually correspond to the entries of D from this work, and not those of \tilde{D} .

It is interesting to consider the conditions that must be satisfied to obtain a diagonal state $|B\rangle_{\pm} = \frac{1}{\sqrt{2}}(|2_1, 0_2\rangle \pm |0_1, 2_2\rangle)$, or an antidiagonal state $|A\rangle = |1_1, 1_2\rangle$.

The diagonal case is achieved when $D_{12} = 0$. This gives rise to two possibilities. First, $|\eta_1| = |\eta_2|$, and $\phi_1 = \phi_2 + 2\pi(m + 1/2)$ with $m \in \mathbb{Z}$ —this is identical to the

condition found in Sec. IV B 2. Second, $z = \pi m/C_0$, with $m \in \mathbb{Z}$.

From Eqs. (46a) and (46c), we can see that $D_{11} = -D_{22}$. This implies that regardless of which diagonal condition is met, only the antisymmetric diagonal state $|B\rangle_-$ is achievable, and Fock states such as $|2_1, 0_2\rangle$ or $|0_1, 2_2\rangle$ are not possible. It is worth noting that the first condition, found in Sec. IV B 2, offers the advantage of being position independent, while the second condition is compatible with any injection profile.

On the other hand, an antidiagonal state requires $D_{11} = D_{22} = 0$. This is only true when $|\eta_1| = |\eta_2|$, $\phi_1 - \phi_2 = 2\pi m$, and $z = \pi(2m + 1)/(2C_0)$ with $m \in \mathbb{Z}$. Therefore, the realization of an antidiagonal state is subject to a position-dependent condition.

B. Solution for three waveguides

For a homogeneous three-waveguide array, the relevant entries of the matrix \tilde{D} are given as follows

$$\begin{aligned} \tilde{D}_{11} &= \frac{i}{16\sqrt{2}C_0} [4C_0z(3\eta_1 - 2\eta_2 + 3\eta_3) \\ &\quad + 8\sqrt{2}(\eta_1 - \eta_3) \sin(\sqrt{2}C_0z) \\ &\quad + \sqrt{2}(\eta_1 + 2\eta_2 + \eta_3) \sin(2\sqrt{2}C_0z)], \end{aligned} \quad (47a)$$

$$\begin{aligned} \tilde{D}_{12} = \tilde{D}_{21} &= \frac{-1}{2C_0} \sin^2\left(\frac{C_0z}{\sqrt{2}}\right) [3\eta_1 + 2\eta_2 - \eta_3 \\ &\quad + (\eta_1 + 2\eta_2 + \eta_3) \cos(\sqrt{2}C_0z)], \end{aligned} \quad (47b)$$

$$\begin{aligned} \tilde{D}_{13} = \tilde{D}_{31} &= i \frac{\eta_1 + 2\eta_2 + \eta_3}{16C_0} [-4C_0z \\ &\quad + \sqrt{2} \sin(2\sqrt{2}C_0z)], \end{aligned} \quad (47c)$$

$$\begin{aligned} \tilde{D}_{22} &= \frac{i}{8\sqrt{2}C_0} [-4C_0z(\eta_1 - 2\eta_2 + \eta_3) \\ &\quad + \sqrt{2}(\eta_1 + 2\eta_2 + \eta_3) \sin(2\sqrt{2}C_0z)], \end{aligned} \quad (47d)$$

$$\begin{aligned} \tilde{D}_{23} = \tilde{D}_{32} &= \frac{-1}{2C_0} \sin^2\left(\frac{C_0z}{\sqrt{2}}\right) [-\eta_1 + 2\eta_2 + 3\eta_3 \\ &\quad + (\eta_1 + 2\eta_2 + \eta_3) \cos(\sqrt{2}C_0z)], \end{aligned} \quad (47e)$$

$$\begin{aligned} \tilde{D}_{33} &= \frac{i}{16\sqrt{2}C_0} [4C_0z(3\eta_1 - 2\eta_2 + 3\eta_3) \\ &\quad + 8\sqrt{2}(\eta_3 - \eta_1) \sin(\sqrt{2}C_0z) \\ &\quad + \sqrt{2}(\eta_1 + 2\eta_2 + \eta_3) \sin(2\sqrt{2}C_0z)]. \end{aligned} \quad (47f)$$

Similarly, the elements of \tilde{D} are consistent with those found by Belsley et al. [16]. We can study again the requirements for diagonal and antidiagonal states. This time, three equations must be satisfied in order to obtain a diagonal state, resulting in $|\eta_1| = |\eta_2| = |\eta_3|$, $\phi_1 - \phi_2 = 2\pi(m + \frac{1}{2})$, and $\phi_1 - \phi_3 = 2\pi m$, with $m \in \mathbb{Z}$. This result is identical to the condition found in Sec. IV B 2, and therefore produces a state with alternating phases—that is, $|B\rangle = \frac{1}{\sqrt{3}}(|2_1, 0_2, 0_3\rangle - |0_1, 2_2, 0_3\rangle + |0_1, 0_2, 2_3\rangle)$.

For an antidiagonal state there are two possible systems of equations. One of these systems has no solutions, whereas the other has an infinite number of solutions, subject only to the constraints $|\eta_1| = |\eta_3|$, $|\eta_2| = 0$, $\phi_1 - \phi_3 = 2\pi(m + \frac{1}{2})$, and $z = \frac{\pi}{\sqrt{2}C_0}m$, with $m \in \mathbb{Z}$. Although this condition is verified at certain positions, it also implies that $\tilde{D}_{13} = 0$. Thus, it is not possible to achieve a Dicke state such as $|1_1, 1_2, 0_3\rangle + |0_1, 1_2, 1_3\rangle + |1_1, 0_2, 1_3\rangle$. However, the state $|A\rangle = |1_1, 1_2, 0_3\rangle + |0_1, 1_2, 1_3\rangle$ is realizable.

The results presented so far for two, and three waveguides for a homogeneous coupling profile are consistent with what has been reported elsewhere [16]. This is important for checking the validity of our method.

C. Injection in one waveguide

Consider the situation when only the l th waveguide is injected into a homogeneous array—that is, with $C_j = C_0$. In that case, the elements of the matrix K are easier to calculate compared to the general case. If N is odd and $l = (N + 1)/2$ —that is, the center waveguide—then, the even rows and columns of K vanish. This implies that, in the supermodes basis, only odd supermodes participate in the evolution, as reported elsewhere [18].

Now, we introduce the correlation matrix Γ , associated with an output state $|\Psi\rangle$, with entries defined as $\Gamma_{kq} = |\langle \dots, 1_k, \dots, 1_q, \dots | \Psi \rangle|^2 / \langle \Psi | \Psi \rangle$ for $k \neq q$, and $\Gamma_{kk} = |\langle \dots, 2_k, \dots | \Psi \rangle|^2 / \langle \Psi | \Psi \rangle$ for the diagonal entries. In terms of the entries of the matrix D , we can write the general expression $\Gamma_{kq} = (2 - \delta_{kq})|D_{kq}|^2 / \sum_{i,j=1}^N |D_{ij}|^2$. Particularly, for $k \neq q$, Γ_{kq} corresponds to the probability of detecting exactly one photon at the waveguide k , and the other at the waveguide q . In addition, Γ_{kk} gives the probability of detecting both photons at the waveguide k [28]. On the other hand, we define the normalized expectation value of $\hat{N}_j = \hat{A}_j^\dagger \hat{A}_j$ —the number operator corresponding to the j th waveguide—as $n_j = \langle \hat{N}_j \rangle / \sum_{k=1}^N \langle \hat{N}_k \rangle = \sum_{k=1}^N (1 + \delta_{jk})|D_{jk}|^2 / [\sum_{n,m=1}^N (1 + \delta_{nm})|D_{nm}|^2]$.

In the following, we consider the injection of one waveguide in the middle of an odd ANW, and focus on what we call the border-free region—within which the borders of the array have negligible influence in the propagation. Here, we define the so-called border-free region as the interval starting from $z = 0$ until the position at which either $n_1(z) = 10^{-3}$ or $n_N(z) = 10^{-3}$.

Moreover, the spreading of the propagation is given by the standard deviation $\sigma = [\sum_{j=1}^N j^2 n_j - (\sum_{j=1}^N j n_j)^2]^{1/2}$, in which the n_j defined above is used as the corresponding probability distribution. In an array with an odd number of waveguides, it is convenient to define the center waveguide as $j = 0$, so that the second sum in the standard deviation vanishes.

It is mentioned in the literature [28] that a linear array exhibits a quantum random walk that spreads bal-

listically. That is, the standard deviation is proportional to the propagation parameter—which in this case corresponds to z . If this were true for an ANW, in principle, one could calculate the standard deviation analytically, and prove that it is proportional to z within the region where the borders have negligible influence.

Before trying to perform a general analytic calculation, we first examined a specific case. Particularly, we analyzed numerically the derivative $d \ln \sigma / d \ln z$ and its dependence with respect to the propagation parameter. Note that for a spreading of the form $\sigma = Az^n$, with A and n constants, the derivative $d \ln \sigma / d \ln z$ would correspond to the exponent n . If the propagation were ballistic, n would be equal to one within the border-free region. This was studied by performing a simulation of an array with $N = 65$ waveguides. For this simulation, the numerical parameters were $C_0 = 250 \text{ m}^{-1}$, $g = 70 \text{ W}^{-1/2} \text{ m}^{-1}$, and $|\alpha_j|^2 = 0.5 \text{ mW}$ for all j . The values of C_0 , and g used in the calculations are representative of an experimental configuration reported elsewhere [29]. The spatial evolution of the normalized number of photons is shown in Fig. 2a. At the beginning, it is different than zero only for the centermost waveguide. As z increases, it spreads following a quantum random walk, and the border-free region extends until $C_0 z \approx 16$. Although the standard deviation seems fairly linear in Fig. 2b, the derivative $d \ln \sigma / d \ln z$ is not constant. Based on this quantity, the spreading appears to propagate faster than in a ballistic case before $C_0 z \approx 2.5$ (where $\sigma > 1$), and slower afterwards (where $\sigma < 1$). Hence, for the configuration described above, the associated standard deviation does not depend linearly on z . This reveals that, in general, a quantum random walk in an ANW does not exhibit a perfect ballistic propagation.

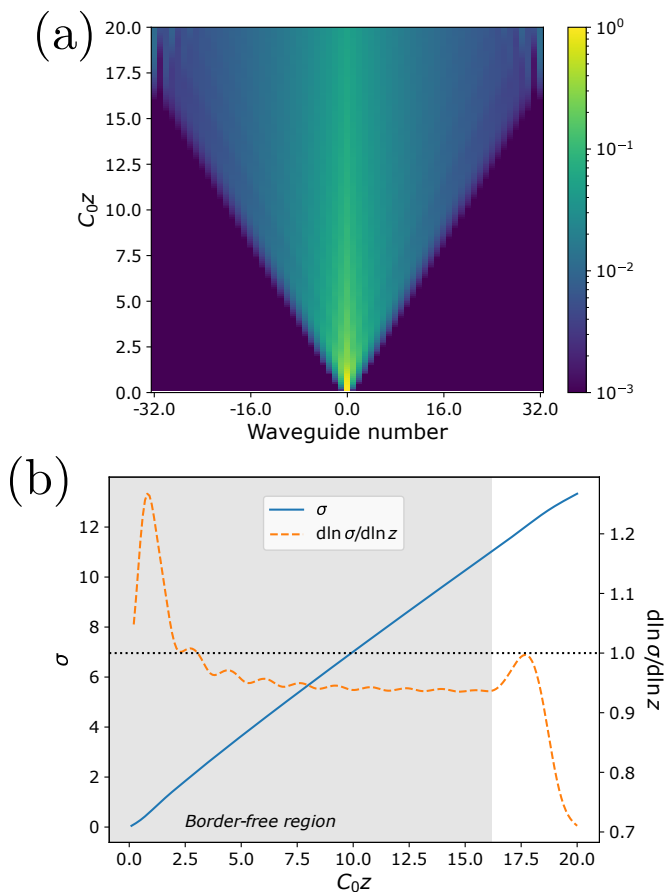


FIG. 2. (a) Propagation in an array of $N = 65$ waveguides when only the center waveguide is injected. (b) Standard deviation σ (solid line, left axis), and the derivative $d \ln \sigma / d \ln z$ (dashed line, right axis) along the propagation. In (a), the color bar indicates the value of the n_j , the propagation distance is described by the dimensionless parameter $C_0 z$, and the waveguide numbers are defined so that $j = 0$ for the center waveguide. In (b), the shadowed area represents the border-free region (described in the main text), and the dotted horizontal line depicts the case of a perfect ballistic propagation—that is, $d \ln \sigma / d \ln z = 1$.

In principle, if the spreading were always ballistic, one should have been able to prove it starting from an analytic solution—such as the one presented in this work. However, as mentioned above, this is not the case.

Regarding quantum random walk studies, it is interesting to point out that they benefit from having a broad border-free region—which is associated with ANWs consisting of a large number of waveguides. In this situation, the analytic solution developed here gives a significant advantage, because it provides an efficient method to calculate an output state, even for large arrays.

VI. INVERSE PROBLEM

A powerful advantage of our method is that, being analytic, it allows to easily invert the problem to determine

the injection profile necessary to produce a given state. In fact, for a general case with an arbitrary coupling profile, the most demanding task—in the calculation of the output state—would be to find the eigenvalues and eigenvectors of the matrix Ω . However, these can be easily obtained numerically, and even analytically in some cases—for example, for a homogeneous profile.

As a proof of concept, we used an optimization method, based on the analytic solution, to determine the injection pump profile required to produce an output state with certain desired characteristics. Particularly, a state with an antidiagonal correlation matrix with equal entries of the form $\Gamma_{qk} = (2 - \delta_{kq})\delta_{k,N+1-q}/N$, and depicted in Fig. 3a.

Since our method is compatible with any coupling profile, we compared between the results obtained for an homogeneous (Fig. 3b), and a parabolic coupling profile (Fig. 3c). The latter is described by $C_j = \sqrt{j(N-j)}C_0/2$. The numerical parameters employed in the simulations were equal to those used in Sec. V C.

In order to quantify how well our results fit the target correlation matrix, we used the similarity $S = (\sum_{i,j=1}^N \sqrt{\Gamma_{ij}\Gamma'_{ij}})^2 / [(\sum_{i,j=1}^N \Gamma_{ij})(\sum_{i,j=1}^N \Gamma'_{ij})]$ between two probability distributions Γ and Γ' [28]. The similarity S takes values between 0 and 1, with $S = 1$ for a perfect overlap between the probability distributions. In general, the closer S is to 1 the more similar are Γ and Γ' .

We obtained $S = 0.692$, and $S = 0.990$, for the homogeneous, and the parabolic coupling profiles, respectively. The details of the optimization method used here, and the obtained injection profiles can be found in Appendix A. In this section, we looked for a state associated with a specific correlation matrix. A similar approach could be used to study the feasibility of achieving a target state with fixed values of \tilde{D}_{ij} (the biphoton states amplitudes), as well as to estimate the corresponding fidelity between the desired and obtained states.

We emphasize the case presented here is a proof of concept. In fact, we do not discard that better values of S could be achieved with a more sophisticated optimization algorithm.

VII. CONCLUSIONS

We used a supermodes approach to obtain an analytic expression for the output states in an ANW for the case of degenerate spontaneous parametric down-conversion, and assuming the undepleted pump approximation. The expression developed here is general for ANWs of any number of waveguides, and coupling profiles. An analytic solution gives physical insight about light propagation in an ANW. A significant advantage of the expression presented here is that it does not require to calculate inverse matrices. In fact, once the eigenvalues and eigenvectors of the coupling matrix are obtained, our method requires

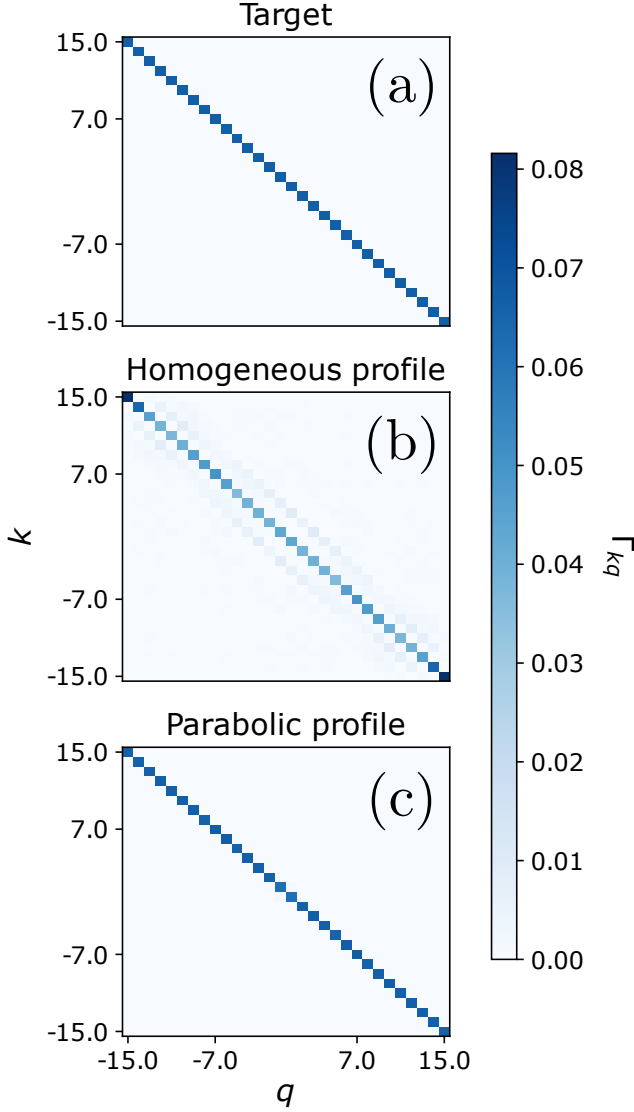


FIG. 3. (a) Target correlation matrix for an array with $N = 30$ waveguides. Panels (a), and (b) depict the obtained correlation matrix after optimization using a homogeneous, and a parabolic coupling profile, respectively. The color bar indicates the value of the correlation matrix entries Γ_{kq} in all cases. The similarity in (b), and (c) is $S = 0.692$, and (c) $S = 0.990$, respectively.

only matrix multiplications, which makes it scalable and highly efficient for numerical implementations. In this regard, we showed proof of concept examples of how to use our method to study quantum random walk, and inversion problems in arrays of nonlinear waveguides. The approach presented in this work could be extended to non-degenerate biphoton states, allowing for the analysis of more general quantum states. Finally, in future work, the analytic and numerical tools developed here could be used to explore interesting problems and phenomena related to arrays of nonlinear waveguides—for example, diffusion regimes in quantum random walks, the introduction of disorder in the pump or coupling profiles, and

the development of improved optimization methods to invert arbitrary output states.

VIII. DATA AVAILABILITY

The data are available from the authors upon reasonable request.

Appendix A: Optimization

In order to obtain a state with an antidiagonal correlation matrix, and with equal entries, we defined the merit function

$$\text{MF}(z, |\eta_1|, \dots, |\eta_N|, \phi_1, \dots, \phi_N) = \sum_{i=1}^N \left[\Gamma_{i, N+1-i} - \frac{(2 - \delta_{i, N+1-i})}{N} \right]^2 + \sum_{i,j=1}^N (1 - \delta_{i, N+1-j}) \Gamma_{ij}^2. \quad (\text{A1})$$

The position, and pump injection profile that minimize this function were determined by performing a minimization method multiple times. For each iteration, if successful, the result of the optimization was used as initial conditions for the next step. Random initial conditions were used otherwise. The reported set of parameters were the ones which gave the lowest value of the merit function.

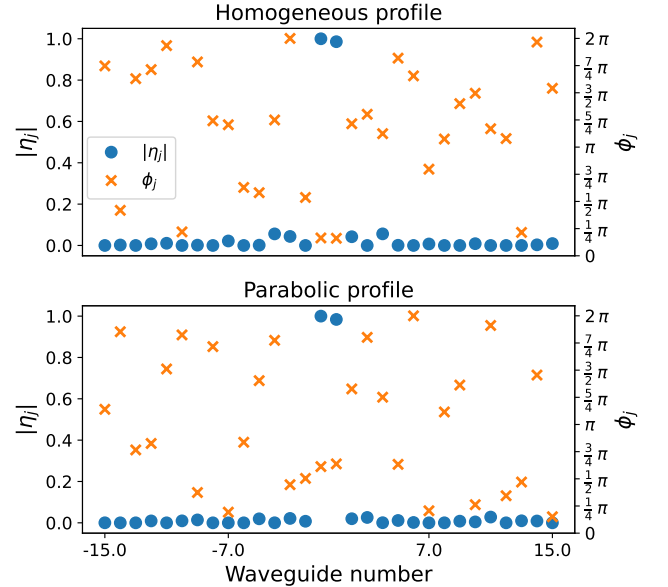


FIG. 4. Amplitudes (circles, left axis) and phases (crosses, right axis) of the pump profile that optimized the merit function using an homogeneous (top panel) and a parabolic (bottom panel) coupling profile.

-
- [1] J. Wang, F. Sciarrino, A. Laing, and M. G. Thompson, Integrated photonic quantum technologies, *Nature Photonics* **14**, 273 (2019).
- [2] D. N. Christodoulides, F. Lederer, and Y. Silberberg, Discretizing light behaviour in linear and nonlinear waveguide lattices, *Nature* **424**, 817 (2003).
- [3] R. Kruse, F. Katschmann, A. Christ, A. Schreiber, S. Wilhelm, K. Laiho, A. Gábris, C. S. Hamilton, I. Jex, and C. Silberhorn, Spatio-spectral characteristics of parametric down-conversion in waveguide arrays, *New Journal of Physics* **15**, 083046 (2013).
- [4] A. S. Solntsev, F. Setzpfandt, A. S. Clark, C. W. Wu, M. J. Collins, C. Xiong, A. Schreiber, F. Katschmann, F. Eilenberger, R. Schiek, W. Sohler, A. Mitchell, C. Silberhorn, B. J. Eggleton, T. Pertsch, A. A. Sukhorukov, D. N. Neshev, and Y. S. Kivshar, Generation of nonclassical biphoton states through cascaded quantum walks on a nonlinear chip, *Physical Review X* **4**, 031007 (2014).
- [5] J. Herec, J. Fiurášek, and L. Mišta, Entanglement generation in continuously coupled parametric generators, *Journal of Optics B: Quantum and Semiclassical Optics* **5**, 419 (2003).
- [6] A. Rai and D. G. Angelakis, Dynamics of nonclassical light in integrated nonlinear waveguide arrays and generation of robust continuous-variable entanglement, *Physical Review A* **85**, 052330 (2012).
- [7] C. S. Hamilton, R. Kruse, L. Sansoni, C. Silberhorn, and I. Jex, Driven quantum walks, *Physical Review Letters* **113**, 083602 (2014).
- [8] D. Barral, M. Walschaers, K. Bencheikh, V. Parigi, J. A. Levenson, N. Treps, and N. Belabas, Versatile photonic entanglement synthesizer in the spatial domain, *Physical Review Applied* **14**, 044025 (2020).
- [9] D. Leykam, A. S. Solntsev, A. A. Sukhorukov, and A. S. Desyatnikov, Lattice topology and spontaneous parametric down-conversion in quadratic nonlinear waveguide arrays, *Physical Review A* **92**, 033815 (2015).
- [10] C. Doyle, W.-W. Zhang, M. Wang, B. A. Bell, S. D. Bartlett, and A. Blanco-Redondo, Biphoton entanglement of topologically distinct modes, *Physical Review A* **105**, 023513 (2022).
- [11] Y. F. Bai, P. Xu, L. L. Lu, M. L. Zhong, and S. N. Zhu, Two-photon anderson localization in a disordered quadratic waveguide array, *Journal of Optics* **18**, 055201 (2016).
- [12] Y. Yang, P. Xu, L. L. Lu, and S. N. Zhu, Manipulation of a two-photon state in a $\chi^{(2)}$ -modulated nonlinear waveguide array, *Physical Review A* **90**, 043842 (2014).
- [13] N. Gisin and R. Thew, Quantum communication, *Nature Photonics* **1**, 165 (2007).
- [14] P. Kok, W. J. Munro, K. Nemoto, T. C. Ralph, J. P. Dowling, and G. J. Milburn, Linear optical quantum computing with photonic qubits, *Reviews of Modern Physics* **79**, 135 (2007).
- [15] D.-H. Kim, S. Hong, Y.-S. Kim, Y. Kim, S.-W. Lee, R. C. Pooser, K. Oh, S.-Y. Lee, C. Lee, and H.-T. Lim, Distributed quantum sensing of multiple phases with fewer photons, *Nature Communications* **15**, 10.1038/s41467-023-44204-z (2024).
- [16] A. Belsley, T. Pertsch, and F. Setzpfandt, Generating path entangled states in waveguide systems with second-order nonlinearity, *Optics Express* **28**, 28792 (2020).
- [17] Y. He, S. Xia, D. Leykam, and Z. Chen, Optimizing biphoton generation via reconfigurable nonlinear waveguide arrays based on scattering tensor, *Optics Express* **32**, 32244 (2024).
- [18] D. Barral, M. Walschaers, K. Bencheikh, V. Parigi, J. A. Levenson, N. Treps, and N. Belabas, Quantum state engineering in arrays of nonlinear waveguides, *Physical Review A* **102**, 043706 (2020).
- [19] J. Noda, M. Fukuma, and O. Mikami, Design calculations for directional couplers fabricated by Ti-diffused LiNbO₃ waveguides, *Applied Optics* **20**, 2284 (1981).
- [20] M. Toren and Y. Ben-Aryeh, The problem of propagation in quantum optics, with applications to amplification, coupling of em modes and distributed feedback lasers, *Quantum Optics: Journal of the European Optical Society Part B* **6**, 425 (1994).
- [21] J. Liñares, M. C. Nistal, and D. Barral, Quantization of coupled 1d vector modes in integrated photonic waveguides, *New Journal of Physics* **10**, 063023 (2008).
- [22] Y. Ben-Aryeh and S. Serulnik, The quantum treatment of propagation in non-linear optical media by the use of temporal modes, *Physics Letters A* **155**, 473 (1991).
- [23] N. Quesada and J. E. Sipe, Effects of time ordering in quantum nonlinear optics, *Physical Review A* **90**, 063840 (2014).
- [24] E. Kapon, J. Katz, and A. Yariv, Supermode analysis of phase-locked arrays of semiconductor lasers: erratum, *Optics Letters* **9**, 318 (1984).
- [25] N. K. Efremidis and D. N. Christodoulides, Revivals in engineered waveguide arrays, *Optics Communications* **246**, 345 (2005).
- [26] M. Reck, A. Zeilinger, H. J. Bernstein, and P. Bertani, Experimental realization of any discrete unitary operator, *Physical Review Letters* **73**, 58 (1994).
- [27] Y.-C. Meng, Q.-Z. Guo, W.-H. Tan, and Z.-M. Huang, Analytical solutions of coupled-mode equations for multiwaveguide systems, obtained by use of chebyshev and generalized chebyshev polynomials, *Journal of the Optical Society of America A* **21**, 1518 (2004).
- [28] A. Peruzzo, M. Lobino, J. C. F. Matthews, N. Matsuda, A. Politi, K. Poulios, X.-Q. Zhou, Y. Lahini, N. Ismail, K. Wörhoff, Y. Bromberg, Y. Silberberg, M. G. Thompson, and J. L. O'Brien, Quantum walks of correlated photons, *Science* **329**, 1500 (2010).
- [29] D. Barral, V. D'Auria, F. Doutre, T. Lunghi, S. Tanzilli, A. Petronella Rambú, S. Tascu, J. Ariel Levenson, N. Belabas, and K. Bencheikh, Supermode-based second harmonic generation in a nonlinear interferometer, *Optics Express* **29**, 37175 (2021).